= 1.08 Å) and introduced in the final structure factor calculations. The final cycles of refinement were carried out on the basis of 201 (5) and 176 (10) variables; after the last cycles, no parameters shifted by more than 1.49 (5) and 1.20 (10) esd. The biggest remaining peak (close to the Pd atom) in the final difference map was equivalent to about 1.08 (5) and 0.81 (10) e/Å^3. In the final cycles of refinement a weighting scheme, $w = K[\sigma^2(F_o) + gF_o^2]^{-1}$, was used; at convergence, the K and g values were 1.019 and 0.0041 for 5 and 0.5856 and 0.0062 for 10, respectively. The analytical scattering factors, corrected for the real and imaginary parts of anomalous dispersions, were taken from ref 32. All calculations were carried out on the CRAY X-MP/12 computer of the Centro di Calcolo Elettronico Interuniversitario dell'Italia Nord-Orientale (CINECA, Casalecchio Bologna) and on the GOULD POWERNODE 6040 of the Centro di Studio per la Strutturistica Diffrattometrica del CNR, Parma, with use of the SHELX-76 and SHELXS-86 systems of crystallographic computer programs.[33] The final atomic coordinates for the non-hydrogen atoms for 5 and 10 are given in Tables IV and V, respectively. The atomic coordinates of the hydrogen atoms are given in Tables SI (5) and SII (10) and the thermal parameters in Tables SIII (5) and SIV (10) of the supplementary material.

Acknowledgment. We thank the CNR (Progetto Finalizzato Chimica Fine II) and the Public Education Ministry for financial support.

Registry No. 1, 135973-06-7; **2a**, 135973-08-9; **2b**, 135973-09-0; 3, 135973-13-6; 4, 135973-10-3; 5 (isomer 1), 135973-11-4; 5 (isomer 2), 136031-57-7; 6, 135973-12-5; 9, 135973-14-7; 10, 135973-15-8; 10·CH_2Cl_2, 135973-17-0; 11, 135973-16-9; $[(C_8H_{12})Ru(\mu\text{-}Cl)]_2$, 12092-47-6; Ph_2PPy, 37943-90-1; $[Rh_2(Ph_2PPy)_2(\mu\text{-}CO)Cl_2]$, 75361-61-4; CO, 630-08-0; *cis*-$[Pd(^tBuNC)_2Cl_2]$, 34710-33-3; $[Pd[CH_2C(CH_3)CH_2]Cl]_2$, 12081-18-4; $[Pd(C_8H_{12})Cl_2]$, 12107-56-1; $[Pd(PhCN)_2Cl_2]$, 14220-64-5; *t*-BuNC, 7188-38-7.

Supplementary Material Available: Tables of hydrogen atom coordinates (Tables SI and SII), thermal parameters for the non-hydrogen atoms (Tables SIII and SIV), and bond distances and angles (Tables SV and SVI) (8 pages); a listing of observed and calculated structure factors (Tables SVII and SVIII) (19 pages). Ordering information is given on any current masthead page.

(32) *International Tables for X-Ray Crystallography*; Kynoch Press: Birmingham, England, 1974; Vol. IV.
(33) Sheldrick, G. M. SHELX-76, *Program for crystal structure determination*, Univesity of Cambridge, England, 1976; SHELXS-86, *Program for the solution of crystal structures*, University of Göttingen, 1986.

Catalytic Disproportionation of Aldehydes with Ruthenium Complexes

Naim Menashe and Youval Shvo*

School of Chemistry, Raymond and Beverly Sackler Faculty of Exact Sciences, Tel Aviv University, Tel Aviv 69978, Israel

Received February 8, 1991

It was discovered that the ruthenium complex $[(C_4Ph_4COHOCC_4Ph_4)(\mu\text{-}H)][(CO)_4Ru_2]$ (2), as well as other isostructural Ru complexes, in the presence of a catalytic amount of formic acid, catalyzes the homogeneous bimolecular disproportionation reaction of aldehydes to give esters: $2RCHO \rightarrow RCOOCH_2R$. The reaction was found to be general and compatible with a variety of aliphatic and aromatic aldehydes and can be carried out in the presence or absence of solvent under mild conditions. It is characterized by an excellent efficiency with an initial turnover frequency reaching 5000 h^{-1}, a measured overall turnover number of ca. 20 000, and high conversion, yield, and selectivity. Increasing the electron density on the metal and the ligand was found to accelerate the reaction. Kinetic studies indicate that the rate = k[catalyst]$^{1/2}$[aldehyde]. The rate also depends on the initial formic acid concentration. A stoichiometric reaction of complex 2 with formic acid, monitored by infrared spectroscopy, shed light on the identity of the active catalytic species. No kinetic isotope effect could be detected by using PhCDO and DCOOD as reactants. Consequently, a mechanism and a detailed catalytic cyle for the bimolecular transformation of aldehydes to esters were proposed.

Introduction

Several years ago we reported that primary alcohols undergo oxidative coupling to esters using dodecacarbonyltriruthenium(0) as a catalyst.[1] Later, Murahashi et al.[2] reported a similar reaction using $H_2Ru(PPh_3)_4$ as a catalyst. In both works[1,2] the oxidative coupling was found to proceed in the presence and absence of H acceptors. Our experimental observations, in particular the persistence throughout the reaction period of a steady-state concentration of aldehyde,[1] led us to propose a reaction sequence that may account for the chemical transformations of the organic components (Scheme I; the role of the catalyst is omitted).

Scheme I

$$RCH_2OH + Ph_2C_2 \rightarrow RCHO + PhCH{=}CHPh \quad (1)$$

$$RCHO + RCH_2OH \rightleftharpoons RCH(OH)OCH_2R \quad (2)$$

$$RCH(OH)OCH_2R + Ph_2C_2 \rightarrow RCOOCH_2R + PhCH{=}CHPh \quad (3)$$

While reactions 1 and 3 definitely require a catalyst, reaction 2 is a simple aldehyde–hemiacetal equilibrium system. The most effective H acceptor was found to be diphenylacetylene, which was irreversibly reduced to

(1) (a) Blum, D.; Reshef, Y.; Shvo, Y. *Tetrahedron Lett.* **1981**, *22*, 1591. (b) Blum, Y.; Shvo, Y. *J. Organomet. Chem.* **1984**, *263*, 93. (c) Blum, Y.; Shvo, Y. *J. Organomet. Chem.* **1985**, *282*, C7.
(2) (a) Murahashi, S. I.; Naota, T.; Ito, K.; Maeda, Y.; Taki, H. *J. Org. Chem.* **1987**, *52*, 4319. (b) Murahashi, S. I.; Naota, T.; Ito, K.; Maeda, Y.; Taki, H. *Tetrahedron Lett.* **1981**, *22*, 5327.

0276-7333/91/2310-3885$02.50/0

Table I. Disproportionation of Aldehydes—Experimental Data

$2RCH_2CHO \rightarrow RCH_2COOCH_2R$

aldehyde	amt of aldehyde, mmol	amt of catalyst,[a] mmol	temp, °C	init TF[b]	TN[c]	Hr	% conv[d]
valeraldehyde	314	0.016	65	5390	19600	5.5	100
isobutyraldehyde	314	0.016	65	3200	9800	11.0	50
pivaldehyde	222	0.016	65	1050	5550	23.0	40
nonanal	150	0.025	65	2510	5700	2.0	95
decanal	147	0.025	65	3400	5700	3.0	97
dodecanal	250	0.025	65	1990	10000	5.0	100
phenylacetaldehyde	250	0.025	65	3400	9000	7.0	90
benzaldehyde	125	0.025	65	880	4000	10.0	80
benzaldehyde	125	0.025	100	4330	4500	4.5	90
p-chlorobenzaldehyde	125	0.025	100	5310	3750	5.0	75
p-methoxybenzaldehyde	125	0.020	100	2030	2500	24.0	50
m-phenoxybenzaldehyde	150	0.025	100	4140	3600	7.0	60
m-phenoxybenzaldehyde	25	0.025	100	1500	950	3.5	95
furfural	25	0.025	100	760	800	6.0	80

[a] Catalyst: $[(C_4Ph_4COHOCC_4Ph_4)(\mu\text{-}H)][(CO)_4Ru_2]$ (**2**). Cocatalyst: HCOOH 10 mol % (based on the aldehyde). [b] (Moles of aldehyde reacted)/(moles of catalyst used)/(hour), measured during the first hour of the reaction where the rates were constant. [c] (Total moles of aldehyde reacted)/(moles of catalyst used) at the specified reaction time and conversion. [d] Calculated from the calibrated areas of the GC signals of the aldehydes and esters.

stilbene.[1] Surprisingly, in the above reaction, diphenylacetylene was found[3] to have a dual role acting both as an H acceptor (Scheme I) and most importantly as a reactant in an initial Ru complex formation reaction according to eq 4. Further reaction of **1** (in situ) leads to the formation of complex **2**, which was eventually isolated,[3] characterized,[4] (X-ray), and found to act as the catalyst, or more accurately, still as a catalyst precursor (eq 5). Nevertheless, **2** can now be prepared independently in good yield[4] and it is the catalyst of choice for further experimental work. (The phenyl substituents on the rings are omitted for clarity in eqs 4 and 5.)

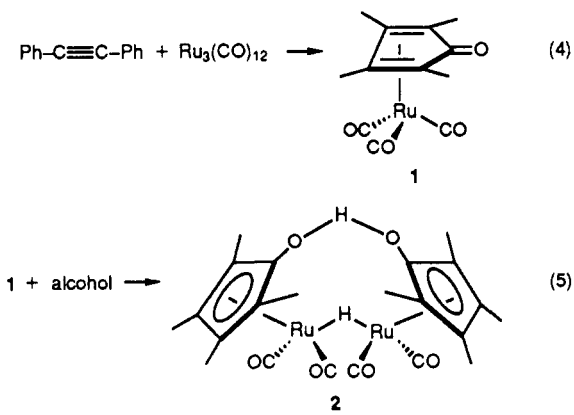

Results and Discussion

The subject of the present report is based on the finding that aldehydes in the presence of **2** undergo a clean catalytic disproportionation reaction (eq 6). Since this is an

$$RCHO + RCHO \rightarrow RCOOCH_2R \qquad (6)$$

overall disproportionation reaction, no H acceptor is required and no coproducts, viz. stilbene (Scheme I), are formed. It is noted that while Scheme I is an overall four-electron oxidation process, the aldehyde and the ester functionalities in reaction 6 are in the same formal oxidation state.

Equation 6 represents a reaction that, when conducted in the presence of alcoholates of alkaline- and alkaline-earth-metal salts, is known as the Tishchenko reaction.[5] In most cases good results are obtained, but some aliphatic aldehydes may undergo undesirable aldol and related side reactions. Boric acid catalyzed Tishchenko type reactions require high temperatures and result in low yields of esters.[6] Limited information exists regarding transition-metal-catalyzed Tischenko type reactions. Disodium tetracarbonylferrate at room temperature catalyzes the transformation of aromatic aldehydes to esters in good yield but with low turnover frequencies.[7] $LiWO_2$ promotes both Tishchenko and Claisen–Tishchenko reactions of aldehydes, resulting in nonselective reactions with aliphatic aldehydes but showing good selectivity toward the formation of esters from aromatic aldehydes.[8] In a study[9] that is most relevant to the present work, $RuH_2(PPh_3)_4$ as well as other hydridoruthenium complexes was found to catalyze reaction 6 with both aliphatic and aromatic aldehydes at convenient temperatures. The conversions and yields are very good, and medium turnover numbers, in the range of a few hundreds of cycles, were realized. The reaction was highly sensitive to traces of water and acid. Two plausible mechanistic routes were proposed by the authors, both of which differ from the present one (vide infra).

In the presence of a catalytic amount of **2**, reaction 6 was found to be an efficient process, provided a catalytic amount of alcohol is present in the reaction solution. Thus, butyraldehyde in the presence of catalytic quantities of **2** and *n*-butanol gives rise to rapid formation of *n*-butyl butyrate. Although the reaction is fast and quantitative, its general practical usage is constrained by the availability of both an aldehyde and its isostructural alcohol. This problem has now been circumvented by reducing a catalytic quantity of aldehyde to alcohol in situ, in a simple manner, without formation of coproducts. The reaction is based on a recent finding that formic acid is a good hydrogen donor in the presence of **2**. Thus, an aldehyde, formic acid (5–10 mol %), and a catalytic amount of **2**

(3) Blum, Y.; Shvo, Y. *Isr. J. Chem.* **1984**, *24*, 144.
(4) Shvo, Y.; Czarkie, D.; Rahamim, Y.; Chodosh, D. F. *J. Am. Chem. Soc.* **1986**, *108*, 7400.
(5) Tishchenko, W. *Zh. Fiz. Khim.* **1906**, *38*, 355. March, J. *Advanced Organic Chemistry*, 3rd ed.; Wiley Interscience: New York, 1985; p 1119.
(6) Stapp, P. R. *J. Org. Chem.* **1973**, *38*, 1433.
(7) Yamashita, M.; Watanabe, Y.; Mitsudo, T. *Bull. Chem. Soc. Jpn.* **1976**, *49*, 3597.
(8) Villacorta, G. M.; Fillipo, J. S. *J. Org. Chem.* **1983**, *48*, 1151.
(9) Ito, T.; Horino, H.; Koshiro, Y.; Yamamoto, A. *Bull. Chem. Soc. Jpn.* **1982**, *55*, 504.

(0.001–0.0002 mol %), in the presence or absence of solvent, generate esters in an extremely efficient manner. In a control eperiment, no reaction was found to take place upon omitting the catalyst. A typical reaction profile is presented in Figure 1.

The results of our experiments and the relevant experimental data are presented in Table I. In order to demonstrate the practicality of this reaction, the experiments were carried out on a preparative scale with no solvents, with the substrate-to-catalyst mole ratio reaching ca. 20000, which is equivalent to a catalyst concentration of ca. 100 ppm. The reaction conditions are mild and simple. The high initial turnover frequency indicates a very fast reaction, while the high turnover numbers are indicative of the satisfactory lifetime (stability) of the catalyst. In fact the reaction solutions are homogeneous and show no sign of catalyst deterioration throughout the reaction period. Indeed, TLC monitoring of the reaction solution showed the presence of the original complex **2** only.

The reaction is compatible with aliphatic and aromatic aldehydes, and gives good results with furfural, representing heterocyclic aldehydes. Comparing the initial reaction rates of aldehydes with similar molecular weight shows a ca. 5-fold decrease in passing from valeraldehyde to pivaldehyde, and also lower turnover numbers (Table I). Thus, the reaction is not very sensitive to steric effects, allowing the formation of the seriously sterically hindered ester, neopentyl trimethylacetate in 40% yield (Table I). The three fatty alcohol–fatty acid esters, which are difficult to obtain by classical esterification procedures, were readily obtained by the present method, and in high yields. The unique conditions of this reaction allow the preparation of a variety of esters that may otherwise be difficult to prepare (Table I). Benzaldehyde is sluggish at 65 °C, but becomes quite reactive at 100 °C. Electron-withdrawing and -donating groups at the para position of aromatic aldehydes accelerate and retard, respectively, the reaction rate. For unknown reasons, with *p*-methoxybenzaldehyde and *m*-phenoxybenzaldehyde the reaction stops at 50–60% conversion, although there are no signs of catalyst deterioration. When the substrate:catalyst ratio was decreased from 6000 to 1000 the reaction was driven to 95% conversion in 3.5 h.

The transformation depicted in eq 6 can be described by reactions 7–10 (Scheme II). For simplicity, M and MH_2 represent reduced and oxidized catalytic organometallic

Scheme II

$$HCOOH + M \rightarrow MH_2 + CO_2 \quad (7)$$

$$MH_2 + RCHO \rightleftharpoons RCH_2OH + M \quad (8)$$

$$RCH_2OH + RCHO \rightleftharpoons RCH(OH)OCH_2R \quad (9)$$

$$RCH(OH)OCH_2R + M \rightarrow RCOOCH_2R + MH_2 \quad (10)$$

species, respectively, originating, in the reaction solution, from complex **2** (vide infra). Later we will discuss their structural significance and mode of formation. It should be recalled that the initial molar ratio of formic acid: aldehyde is 1:10.

Scheme II is supported by the reaction profile (Figure 1) that clearly indicates a fast formation of *n*-pentyl alcohol right at the onset of the reaction, and in a quantity corresponding to that of the initiallay present formic acid (10 mol %). The above concentration level of the alcohol was sustained throughout the reaction period (Figure 1), in agreement with Scheme II. Since all the formic acid was consumed at the beginning of the reaction, both reactions 7 and 8 must be essentially quantitative and irreversible,

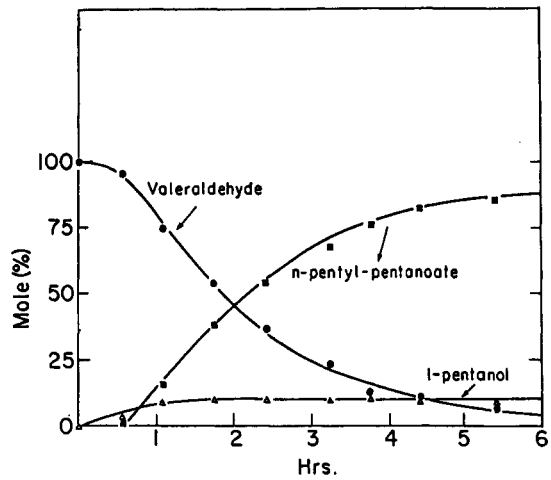

Figure 1. Disproportionation reaction of valeraldehyde. Conditions: [aldehyde] = 1.0 M, [HCOOH] = 0.1 M, [2] = 1×10^{-3} M in toluene at 65 °C.

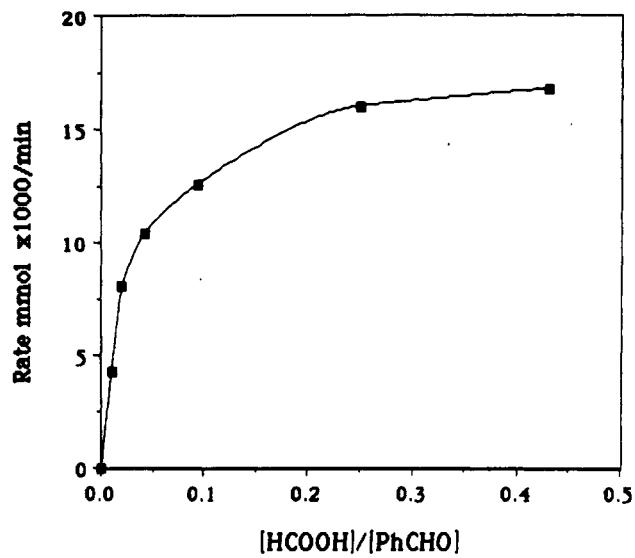

Figure 2. Initial rates of formation of benzyl benzoate with variable quantities of formic acid. Conditions: [PhCHO] = 1.0 M; [2] = 1×10^{-3} M in toluene at 90 °C.

generating the stoichiometric quantity of alcohol. Thus, reactions 7 and 8 may be considered as an independent catalytic initiation cycle accounting for the alcohol formation, the consumption of formic acid, the evolutioan of CO_2, and the fact that practically no ester is being formed at the beginning of the reaction period.

According to eqs 7 and 8 (Scheme II), equivalent molar quantities of M and formic acid are sufficient to make the overall cycle viable. In practice, the quantity of formic acid exceeds many-fold the quantity of the catalyst. Experiments indicate that the overall reaction rate does depend on the initial concentration of formic acid (Figure 2), also beyond the catalyst concentration. Even without added formic acid a very slow reaction was observed. The fact that the stationary level of alcohol concentration, derived from formic acid, does affect the reaction rate is attributed to the participation of the alcohol in the aldehyde–hemiacetal equilibrium (eq 9), thereby affecting the rate of reaction 10, which is associated with the rate-determining step for the overall process (vide infra). The leveling off of Figure 2 at high concentrations of formic acid will be discussed later.

The catalyst structure–reactivity relationship was examined with several new isostructural complexes (Table II). It is evident that ring substitution affects the rates

Table II. Structure Reactivity Relationship[a]

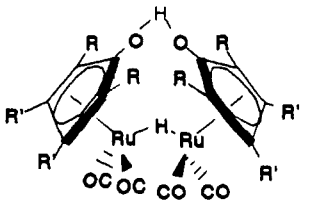

complex	R	R′	10^2 rate, mmol/min
3	phenyl	*p*-methoxyphenyl	2.21
2[4]	phenyl	phenyl	1.50
4	phenyl	*p*-fluorophenyl	1.30
5[4]	phenyl	*p*-chlorophenyl	0.90
6	*p*-chlorophenyl	*p*-chlorophenyl	0.48

[a] Reaction conditions: [catalyst] = 1×10^{-3} M; [PhCHO] = 1.0 M; [HCOOH] = 0.10 M in toluene at 90 °C. Rates are initial, measured during first 90 min of the reaction, and are constant.

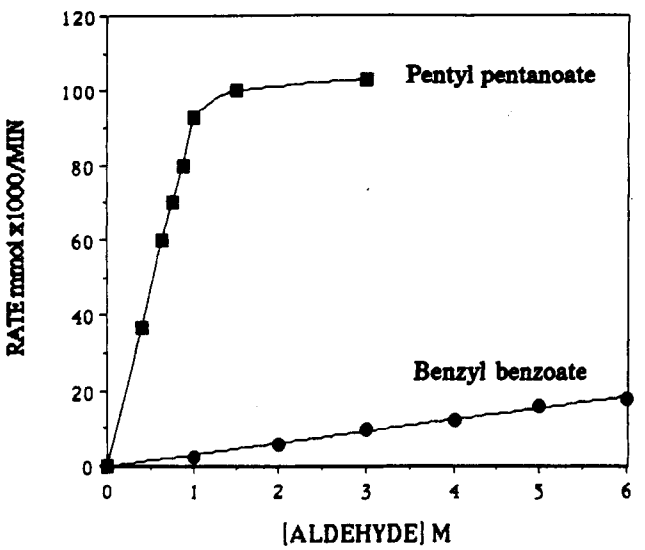

Figure 3. Initial rates of formation of esters using variable concentrations of aldehydes and **2** as a catalyst. Conditions: [**2**] = 10^{-3} M; [HCOOH] = 0.02 M in toluene; temp = 70 °C.

by a moderate overall factor of ca. 5 (maximum). Electron-releasing substituents accelerate the conversion of aldehydes to esters, evidently by increasing the electron density on the cyclopentadienyl ligand (vide infra).

Next we have studied the dependence of the reaction rate on the aldehyde concentration. Different behaviors were noted with the aliphatic and aromatic aldehydes, as depicted in Figure 3. Pentanal is by far more reactive than benzaldehyde, but the reaction rate (initial) of the latter is constant up to a concentration of 6 M. Considering that the concentration of the catalyst (**2**) is only 10^{-3} M, a zero rate order would be expected at much lower benzaldehyde concentration, as with pentanal (Figure 3). Consequently, the active catalytic species does not directly interact with the aldehyde, but rather via an intermediate, most logically, a hemiacetal. It must be concluded that in the case of benzaldehyde, the concentrations of the catalyst and the hemiacetal (α-(benzyloxy)benzyl alcohol) are of the same order of magnitude, while with pentanal the concentration of 1-(pentyloxy)pentan-1-ol (at ca. 1 M pentanal concentration) is by far higher than that of the catalyst. In order to substantiate this conclusion we have measured, by using ^{1}H NMR spectroscopy,[10] the equilibrium constants for the

(10) Bone, R.; Cullis, P.; Wolfenden, R. *J. Am. Chem. Soc.* **1983**, *105*, 1339.

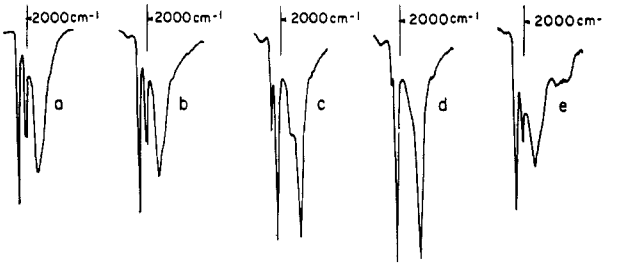

Figure 4. Infrared spectroscopic monitoring of the reaction of **2** in formic acid: (a) **2** (60 mg) in THF (10 mL) at ambient temperature; (b) **2** (60 mg) in THF (10 mL) + formic acid (100 mg) at ambient temperature; (c) after heating sample b at 60 °C for 10 min; (d) after heating sample b at 60 °C for 15 min; (e) 15 min after the addition of PhCHO (1.0 g) to d at ambient temperature.

Scheme III

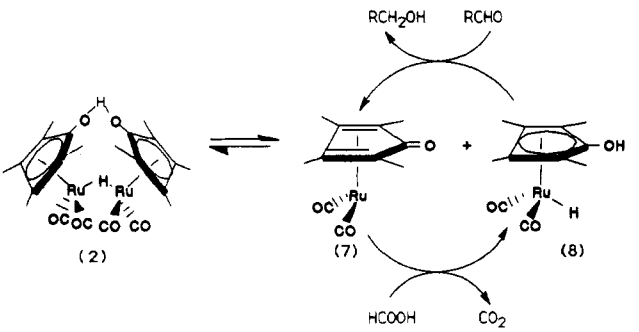

formation of the above two hemiacetals. The constants were determined from the slope of the straight line obtained by plotting (hemiacetal)/(aldehyde) vs (alchol) at 25 °C (equilibration is instantaneous). It was found that for pentanal K(25 °C) = 0.34 M^{-1}, and for benzaldehyde K(25 °C) and K(70 °C) < 0.03 M^{-1}. Since no changes could be detected in the areas of the benzaldehyde and benzyl alcohol NMR signals at both temperatures, the latter K equilibrium value was considered as an upper limit estimate. With the above value (0.03 M^{-1}), it was estimated that, in the experiment described in Figure 5 at 6 M concentration of benzaldehyde, the initial hemiacetal concentration is 3.6×10^{-3} M, indeed in the range of the catalyst concentration (10^{-3} M). The above results prove the following points: (i) hemiacetal is the reactive intermediate that is being oxidized by a catalyst to the ester; (ii) hemiacetalization is an independent reaction, not assisted by the catalyst; (iii) the reaction is first order in the aldehyde.

The molecular structure of M and MH_2 and the reaction mechanism are of interest. It should be pointed out that the starting complex (**2**) does not appear in Scheme II although it was found to be present throughout and at the end of the disproportionation reactions of the various aldehydes, as was determined by TLC and infrared monitoring of the reaction solutions. Although **2** is a 34-electron dimer complex, it should be considered as a catalyst precursor rather than an active catalytic species. The questions now are, how do M and MH_2 originate, what structures do they possess, and what role do they play in the catalysis. To this end, the reaction of **2** in THF with formic acid, but *in the absence of aldehyde*, was examined by monitoring its infrared spectrum (CO stretching vibration region) under several conditions (Figure 4).

While at room temperature complex **2** is stable in the absence or presence of formic acid (Figure 4a,b); at 60 °C a rapid change in the infrared spectrum occurred. The initial three-band spectrum gradually changed (10 min;

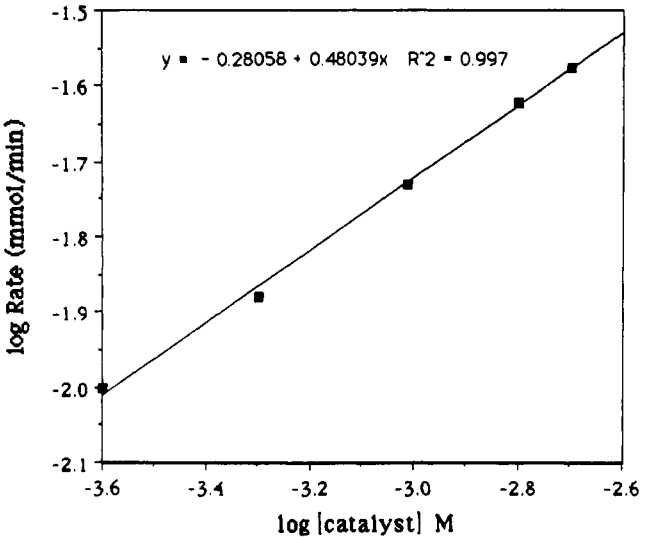

Figure 5. log of rate of formation of benzyl benzoate vs log of concentration of **2**. Conditions: [PhCHO] = 1.0 M in toluene at 90 °C. The individual rates were measured from the straight line portion of the initial rates curves.

Figure 4c) to a clean two-band spectrum (Figure 4d). Upon the addition of benzaldehyde to the this solution, the spectrum instantaneously reverted to that of the starting complex **2** (Figure 4e). The solution of **2** was found to be yellow, while that associated with Figure 4d was colorless.

The above spectral changes lead to the formulation of Scheme III (ring substituents were omitted), the initiation cycle, and the molecular structures of the catalytically active species **7** and **8**. In previous studies,[4] we have established that in solution complex **2** is in equilibrium with its monomeric constituents **7** and **8**, the equilibrium being strongly shifted toward **2**. For the present system, it was important to determine the dependence of the rate (initial) of the disproportionation reaction on the concentration of **2**. The results presented in Figure 5 indicate a reaction order close to $^1/_2$, thus supporting the hypothesis of the dissociation of **2** into two catalytically active particles under the present experimental conditions as described in Scheme III.

We propose that **7**, a 16-electron undetectable species, oxidatively adds hydrogen from formic acid, generating **8**, the infrared-detectable species (two CO bands; Figure 4d). It should be mentioned that **8** was previously[4] obtained by hydrogenation of **2** under pressure and was found to be stable only in solution (colorless). Its formation in the presence of *formic acid* has now been experimentally demonstrated (Figure 4). Thus **7** and **8** are respectively M and MH_2 in Scheme II. (The ability of **8** to instantaneously deliver at room temperature its H atoms to an aldehyde rules out reaction 8 as the rate-determining step of the overall catalytic process).

The above spectral changes also indicate that in the presence of formic acid, the equilibrium presented in Scheme III is strongly shifted toward **8**. In principle, 1 equiv of formic acid is sufficient in order to transform all of **2** into **8**. In practice, the excess formic acid present (with respect to 2) is decomposed via reduction of the aldehyde by the combined action of **8** and **7**, as described in Scheme III, thereby building up the steady-state alcohol concentration and completing the initiation cycle (eq 7 and 8). Scheme III does not carry any information regarding the catalyst–substrate interaction (vide infra).

Complexes **7** and **8** also participate in the propagating cycle (eqs 8–10) whereby an ester is being formed. Before presenting our conception of the overall catalytic cycle, two

Scheme IV

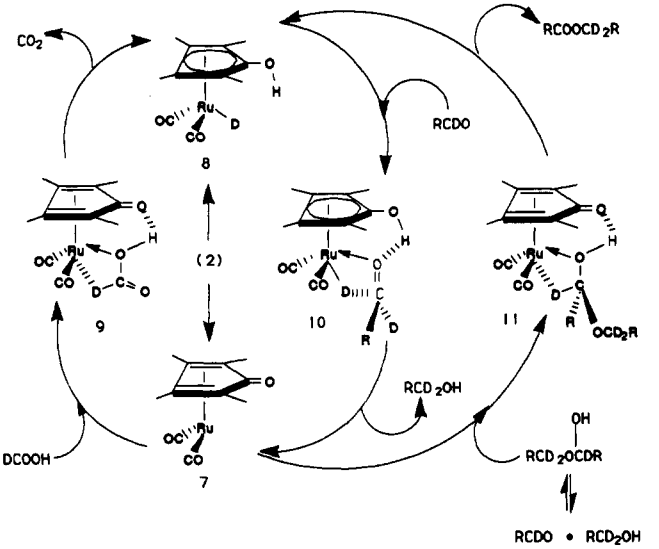

additional experiments will be described: (a) No retardation in the catalysis rate, using DCOOD + PhCDO and **2** as a catalyst, was observed. (b) An experiment that reveals additional participating intermediates and supports the assignment of their molecular structure is described in eq 11.

$$\mathrm{PhCDO + DCOOH} \xrightarrow[-CO_2]{2} \mathrm{PhCD_2OH + PhCOOCD_2Ph} \quad (11)$$

Reaction 11 was stopped when the concentrations of the components were benzaldehyde 1.8%, benzyl alcohol 43.7%, and benzyl benzoate 54.5%, after which the alcohol and the ester were separated by column chromatography. The ^{1}H NMR spectra indicated that the methylenes of both benzyl alcohol and benzyl benzoate were fully deuterated (>99%), as described by eq 11. These results indicate that during catalysis the H and D atoms occupy and retain discrete sites within the various catalytic species and moreover are transferred to the substrates with complete regioselectivity.

On the basis of the results presented hitherto, and in particular on the basis of eq 11, we are proposing in Scheme IV a catalytic cycle for the conversion of aldehydes to esters in the presence of catalytic amounts of **2** and formic acid. Although Scheme IV is presented in conjunction with eq 11 with deuterated starting materials, obviously it is a general scheme applicable to all aldehydes in the presence of formic acid.

The cycle in Scheme IV deserves some explanations and comments: (a) Aside from the two transformations involving the formation of CO_2 and ester, all others are reversible (vide infra). (b) The starting point of the cycle is complex **2** (d_2), which by dissociation generates the previously described **7** and **8**. (c) The left-hand cycle involving **7**–**10** is the initiation cycle that consumes all the formic acid present, thereby generating the steady-state alcohol concentration. (d) The right-hand cycle involving **7**, **11**, **8**, and **10** is the propagation cycle responsible for the oxidation of the hemiacetal. (e) Intermediates **9**–**11** account for the complete deuteration of the alcohol and the ester, as described by eq 11. Thus the regiospecificity in the H–D distribution originates from regiospecific interactions between the particular intermediate complexes **7** and **8** and the corresponding substrates *and lends support in the very structures of these catalytic species.* The implication is that the acidic and hydridic nature of the

Table III. Rate of Ester Formation from Aldehyde-Solvent Effect[a]

	valeraldehyde mmol/min	benzaldehyde mmol/min
toluene	6.5×10^{-2}	5.5×10^{-3}
THF	3.3×10^{-2}	2.8×10^{-3}

[a] Reaction conditions: [aldehyde] = 1.0 M; [HCOOH] = 0.1 M; [2] = 10^{-3} M. Reaction temp = 65 °C; rates measured after 1-h reaction time.

two H atoms in 8 are well defined and preserved under the reaction conditions. All possible reversible steps must also be regiospecific. (f) It is probable that during catalysis the cycle is still in equilibrium with 2, although the reaction solution loses most of its orange color. At the end of the reaction (low concentration of reactants) the system was observed to relax back to 2 (color change, TLC, IR spectroscopy). (g) Alcohol does most probably compete with the hemiacetal for 7, regenerating the aldehyde. Of course this is a degenerate process that does not affect the alcohol:aldehyde ratio and therefore cannote be detected. We have demonstrated the feasibility of this reversible reaction (7 → 10 → 8) by reacting equimolar quantities of nonanal and 1-pentanol in the presence of 2. The two major products obtained at 100% conversion of the nonanal were pentyl nonanoate and pentyl pentanoate (14.5:1). Consequently, pentanal, that gave rise to pentyl pentanoate, must have originated by oxidation (H transfer to nonanal) of the originally present pentanol. The implication of this observed reversibility is that higher concentrations of alcohol should on one hand retard the reaction due to competition of alcohol ahd hemiacetal for 7, while on the other hand accelerate the rate by shifting the equilibrium (eq 9) toward the hemiacetal. In practice, the dependence of the initial disproportionation rate of benzaldehyde on the steady-state concentration of benzyl alcohol (formic acid) is presented in Figure 2. Clearly, a moderation in the reaction rate with increasing alcohol concentration is evident and is attributed to the action of the two opposing effects. (h) As with many catalytic processes involving transition-metal complexes, the ruthenium atom oscillates between two oxidation states, in the present case 0 and II. The unique aspect of the present catalytic system is that no foreign reagent is required in order to modify the oxidation states of the metal atom, thus *both* oxidation states are catalytically productive. (i) Electron-donating groups on the cyclopentadienone ligand, which were found to accelerate the disproportionation reaction (Table II), place extra electron density on the carbonyl oxygen atom of the cyclopentadienyl ligand. This could be verified by comparing the C=O stretching frequency of the cyclopentadienone ruthenium tricarbonyl complexes [2,5-bis-(C_6H_5)-3,4-bis(4-MeO-C_6H_4)C_4CO]Ru$(CO)_3$, ν = 1630 cm^{-1}, and [(4-Cl-C_6H_4)$_4C_4CO$]Ru$(CO)_3$, ν = 1650 cm^{-1}, (see Experimental Section). The enhanced basicity of this oxygen atom promotes a stronger hydrogen bond with the incoming protic substrate, consequently lowering the energy of 11 (Scheme IV). (j) As to the rate-limiting step of the propagation cycle, it is clear that with benzaldehyde the reduction step (eq 8) must be ruled out on the basis of Figure 3. Since the reaction rate depends on both the catalyst and aldehyde concentrations, eq 10 must be associated with the RDS. However, according to Scheme IV, eq 10 is composed of two steps: 7 → 11, a coordination step, and 11 → 8, an oxidative addition of two H atoms.[11] Since no kinetic isotope effect could be detected by using DCOOD and PhCDO, the latter step must be ruled out as the rate-limiting step, leaving the coordination step of the hemiacetal (7 → 11) as a candidate for the RDS of the overall process. Although we have no evidence, it is conceivable that 9 and 11 (and also 7) collapse to the corresponding alkoxide intermediates forming Ru–O and O–H σ bonds such as in 12 and 13, which subsequently undergo

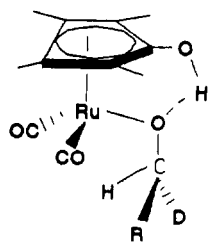

12

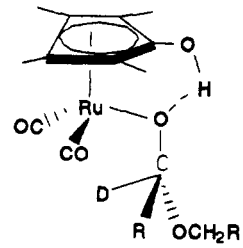

13

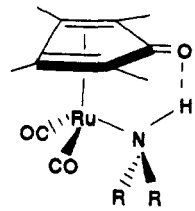

14

a β-elimination process, generating 8 and a carbonyl functionality (ester). Intermediates 9–11, as well as 12 and 13, are characterized by a Ru-coordinated oxygen atom and a pattern of O–H–O interactions. The structures of these hypothetical species find support in the isostructural amine complex 14, which was prepared, isolated, and characterized by X-ray crystallography.[12] The Ru–N (2.214 Å), NH–O (2.848 Å), and O- -H (1.98 Å) bond lengths clearly establish the bonding interactions in 14, which by analogy may also prevail in the intermediates 9–13. Of course an amine complex (isolated) is more stable than its oxygen analogue, which could not be isolated.

Although the preparative coupling reaction of aldehydes is best carried out in the absence of solvent, initial reaction rates were briefly examined in THF and toluene solutions and are presented in Table III.

The decrease in the reaction rate in going from toluene to THF with both aldehydes (ca. 50%) may be attributed to coordination of the latter to the coordinatively unsaturated species 7, the active catalytic species in the RDS (Scheme IV).

Experimental Section

Instruments and Materials. MS–GC analyses were carried out on a Finnigan-Mat Model ITD 800, ion trap detector mass spectrometer. ^1H NMR spectra were recorded on Bruker FT-200-MHz instrument. GC analyses were carried out on Varian instruments Models 3700 and 3300. All aldehydes were distilled and kept under nitrogen before use. Reaction products listed in Table I are known compounds. They were identified by comparison with authentic materials whenever possible, otherwise their identity was established by mass spectral and NMR analyses. The purity of the distilled products was determined by quantitative GC analyses. Alumina with activity II was used for chromatography.

[2,5-(C_6H_5)$_2$-3,4-(4-MeOC_6H_4)$_2C_4CO$]$_2$H(μ-H)$(CO)_4Ru_2$ (3). $Ru_3(CO)_{12}$ (0.639 g, 1.0 mmol), 2,5-diphenyl-3,4-bis(4-methoxyphenyl)cyclopentadienone[13] (1.778 g, 4 mmol), and toluene (10

(11) It is realized that the Ru atoms in 7, 9, and 11 formally carry more than 18 electrons; however some bond breaking and making are implied.

(12) Abed, M.; Goldberg, I.; Stein, Z.; Shvo, Y. *Organometallics* **1988**, *7*, 2054.

(13) Neckers, D. C.; Hauck, G. *J. Org. Chem.* **1983**, *48*, 4691.

mL) were placed in a stainless steel reactor (35 mL). Before the reactor was closed, the content was purged with nitrogen. After heating for 24 h at 150 °C, the reactor was cooled to ambient temperature, the solution was purged with nitrogen to remove dissolved CO gas, and the reactor was closed and reheated at the above temperature for an additional 5 h. After cooling to room temperature, the toluene was removed in vacuo and the residue was dissolved in dichloromethane, which was passed through a silica column. After elution of the starting material with dichloromethane, the product [2,5-diphenyl-3,4-bis(4-methoxyphenyl)cyclopentadienone]tricarbonylruthenium(0) was obtained (70%) as a colorless solid, mp 191 °C dec, having a single TLC spot. Anal. Calcd for $C_{34}H_{24}O_6Ru$: C, 64.86; H, 3.84. Found: C, 65.10; H, 3.92. IR (CH_2Cl_2): ν 2080, 2005, 1630 cm^{-1}. ^1H NMR (C_6D_6): δ 3.04 (s, 6 H), 6.35–7.97 (m, 18 H).

The product obtained above (0.315 g, 0.5 mmol), in acetone (20 mL) and a saturated solution of sodium carbonate (10 mL), was stirred under a nitrogen blanket at room temperature for 30 min. At the end of the reaction (TLC monitoring) the orange reaction solution was neutralized with saturated ammonium chloride solution and most of the acetone was removed in vacuo. The residue was extracted with methylene chloride, which was dried over $MgSO_4$, and filtered, and the solvent was removed in vacuo. The residue was chromatographed on a silica column that was first washed with petroleum ether (60–80), then with a solution of methylene chloride:petroleum ether (1:1) that eluted **3** as an orange solid (75%), mp 210 °C dec, single TLC spot. Anal. Calcd for $C_{66}H_{50}O_{10}Ru_2$: C, 65.77; H, 4.18. Found: C, 66.25; H, 4.45. IR (CH_2Cl_2): ν 2030, 2000, 1970, 1510 cm^{-1}. ^1H NMR ($CDCl_3$): δ −18.47 (s, 1 H), 3.68 (s, 6 H), 6.52–7.12 (m, 17 H). ^{13}C NMR: δ 54.4 (MeO), 88.34 (C2 + C5), 103.8 (C3 + C4), 159.6 (C1), 113.4, 155.1 (phenyls), 202.1 (CO).

[2,5-$(C_6H_5)_2$-3,4-(4-$FC_6H_4)_2C_4CO]_2H(\mu$-H)$(CO)_4Ru_2$ (4). $Ru_3(CO)_{12}$ and 2,5-diphenyl-3,4-bis(4-fluorophenyl)cyclopentadienone[14] were reacted as described above to give [2,5-diphenyl-3,4-bis(4-fluorophenyl)cyclopentadienone]tricarbonylruthenium(0) as a colorless solid, mp 189 °C dec, single TLC spot. Anal. Calcd for $C_{32}H_{18}F_2O_4Ru$: C, 63.47; H, 3.00. Found: C, 63.76; H, 3.15. IR (CH_2Cl_2): ν 2090, 2035, 2020, 1640 cm^{-1}. ^1H NMR (C_6D_6): δ 6.35–7.86 (m).

Complex **4**, an orange solid, mp 220 °C dec, having a single TLC spot, was obtained by treating the above product as described for the isostructural complex **3**. Anal. Calcd for $C_{62}H_{38}F_4O_6Ru_2$: C, 64.36; H, 3.31. Found: C, 64.48; H, 3.35. IR (CH_2Cl_2): ν 2040, 2010, 1980, 1520 cm^{-1}. ^1H NMR: δ −17.9 (s, 1 H), 6.35–7.86 (m). ^{13}C NMR: δ 88.1 (C2 + C5), 103.1 (C3 + C4), 165.2 (C1), 114.9, 134.2 (phenyls), 157.7 (J = 247 Hz, C–F), 201.6 (CO).

[(4-Cl-$C_6H_4)_4C_4CO]_2H(\mu$-H)$(CO)_4Ru_2$ (6). $Ru_3(CO)_{12}$ (0.64 g, 1.0 mmol), bis(4-chlorophenyl)acetylene (0.996 g, 4 mmol), and toluene (10 mL) were heated in a closed stainless steel reactor at 150 °C for 24 h. The reaction mixture was worked up as described above for [2,5-diphenyl-3,4-bis(4-methoxyphenyl)-cyclopentadienone]tricarbonylruthenium(0). There was obtained 0.86 g of [tetrakis(4-chlorophenyl)cyclopentadienone]tricarbonylruthenium(0), orange solid (40%), mp 200 °C dec, pure by TLC. Anal. Calcd for $C_{32}H_{16}Cl_4O_4Ru$: C, 54.33; H, 2.28. Found: C, 54.14; H, 2.38. IR (CH_2Cl_2): ν 2090, 2025, 2020, 1650 cm^{-1}. ^1H NMR ($CDCl_3$): δ 6.95–7.42 (m).

Complex **6**, an orange solid, mp 252 °C dec, pure by TLC, was obtained (79%) upon treating the above complex in actone with aqueous sodium carbonate, as described for **4**. Anal. Calcd for $C_{62}H_{34}Cl_8O_6Ru_2$: C, 54.72; H, 2.52. Found: C, 55.47; H, 2.80. IR (CH_2Cl_2): ν 2040, 2015, 1970, 1520 cm^{-1}. ^1H NMR ($CDCl_3$): δ −15.87 (s, 1 H), 6.92–7.37 (m, 17 H). ^{13}C NMR (THF with external D_2O lock): δ 86.9 (C2 + C5), 103.3 (C3 + C4), 160 (C1), 128.7, 135.2 (phenyls), 201.9 (C0).

General Procedure for the Preparation of Esters from Aldehydes. The following is a typical preparative procedure: A solution of distilled benzaldehyde (21.1 g, 0.199 mol), formic acid (0.915 g, 0.0199 mol) and **2** (27 mg, 0.0252 mmol) was heated under nitrogen at 100 °C for 20 h (97% conversion by GC). The pale yellow homogeneous solution was distilled to give the following fractions: 80 °C/20 mmHg, a mixture of benzaldehyde and benzyl alcohol (0.4 g); 90 °C/1 mmHg, benzyl alcohol (1.51 g); 140 °C/1 mmHg, benzyl benzoate (17.5 g, 83%). The ester (>99% purity by GC) was identified by GC and NMR and mass spectra.

Reactions with Deuterated Compounds. a. PhCDO[15] (2.653 g, 25 mmol), DCOOH[16] (0.345 g, 7.5 mmol) and **2** (27 mg, 0.025 mmol) were heated at 90 °C for 4.5 h. GC analysis of the reaction mixture, w/w %: benzaldehyde 1.8, benzyl alcohol 43.7, benzyl benzoate 54.5. The mixture was separated by chromatography on an alumina column to give, with methylene chloride:pet ether (1:2), benzyl benzoate [^1H NMR ($CDCl_3$): δ 7.2–8.2 (m, 10 H). 5.35 (s, <0.01 H)] and, with methylene chloride, benzyl alcohol [^1H NMR ($CDCl_3$): δ 7.26 (m, 5 H), 4.50 (s, <0.01 H)], both identified by IR and GC analyses.

b. A toluene solution having the composition PhCHO (1 M), HCOOH (0.1 M), and **2** (1.5×10^{-3} M) and a second solution having the above concentrations but of PhCDO and DCOOD, were kept in an oil bath at 90 °C for 1 h. The rates of ester formation were determined by GC analysis from the slopes of the straight lines and were found to be 1.14 and 1.10 mmol/min, respectively; k_H/k_D = 1.

Reaction of Nonanal and Pentan-1-ol. Nonanal (20 mmol), pentan-1-ol (20 mmol), and **2** (0.025 mmol) were heated for 15 min at 90 °C under nitrogen at which time all the nonanal was consumed. The products (molar ratio) pentyl *n*-nonanoate (14.5), pentyl *n*-pentanoate (1), and nonyl *n*-nonanoate (0.3) were identified by MS–GC and quantified by GC analysis. Traces of pentan-1-ol and nonan-1-ol were also present.

Registry No. **2**, 104439-77-2; **3**, 135853-87-1; **4**, 135853-88-2; **5**, 104439-78-3; **6**, 135853-89-3; $H_3C(CH_2)_3COO(CH_2)_3CH_3$, 591-68-4; $(H_3C)_2CHCOO(CH_3)_2$, 617-50-5; $(H_3C)_3CCOO(CH_3)_3$, 16474-43-4; $H_3C(CH_2)_7COO(CH_2)_7CH_3$, 5303-26-4; $H_3C(CH_2)_8C$-$OO(CH_2)_8CH_3$, 42231-48-1; $H_3C(CH_2)_{10}COO(CH_2)_{10}CH_3$, 3658-44-4; $PhCH_2COOCH_2Ph$, 102-16-9; PhCOOPh, 120-51-4; Cl-*p*-$C_6H_4COOC_6H_4$-*p*-Cl, 6961-42-8; MeO-*p*-$C_6H_4COOC_6H_4$-*p*-OMe, 60127-34-6; PhO-*m*-$C_6H_4COOC_6H_4$-*m*-OPh, 3586-16-1; $Ru_3(CO)_{12}$, 15243-33-1; (2-furyl)furan-2-carboxylate, 104939-60-8; pentyl *n*-nonate, 61531-45-1; pentan-1-ol, 71-41-0; 2,5-diphenyl-3,4-bis-(4-methoxyphenyl)cyclopentadienone, 668-29-1; 2,5-diphenyl-3,4-bis(4-fluorophenyl)cyclopentadienone, 56805-29-9; bis(4-chlorophenyl)acetylene, 1820-42-4; [2,5-diphenyl-3,4-bis(4-methoxyphenyl)cyclopentadienone]tricarbonylruthenium(0), 135853-90-6; [2,5-diphenyl-3,4-bis(4-fluorophenyl)cyclopentadienone]-tricarbonylruthenium(0), 135853-91-7; [tetrakis(4-chlorophenyl)cyclopentadienone]tricarbonylruthenium(0), 135853-92-8; benzaldehyde, 100-52-7; nonanal, 28473-21-4; valeraldehyde, 110-62-3; isobutyraldehyde, 78-84-2; pivaldehyde, 630-19-3; decanal, 112-31-2; dodecanal, 112-54-9; phenylacetaldehyde, 122-78-1; *p*-chlorobenzaldehyde, 104-88-1; *m*-methoxybenzaldehyde, 123-11-5; *m*-phenoxybenzaldehyde, 39515-51-0; furfural, 98-01-1; formic acid, 64-18-6.

(14) Cava, M. P.; Narishman, K. *J. Org. Chem.* **1969**, *34*, 3641.

(15) Burgstahler, A. W.; Walker, D. E.; Kuebrich, J. P., Jr.; Schowen, L. *J. Org. Chem.* **1972**, *37*, 127.

(16) Ropp, G. A.; Melton, C. E. *J. Am. Chem. Soc.* **1958**, *80*, 3509.